

Article

Supplementary Materials: Single-Atom Mn Active Site in Triol-Stabilized β -Anderson Manganohexamolybdate for Enhanced Catalytic Activity towards Adipic Acid Production

 Jianhui Luo ^{1,2,+}, Yichao Huang ^{3,+}, Bin Ding ^{1,2}, Pingmei Wang ^{1,2}, Xiangfei Geng ^{1,2}, Jiangwei Zhang ^{3,*} and Yongge Wei ^{3,*}

¹ Research Institute of Petroleum Exploration & Development (RIPED), Petro China, Beijing 100083, China; luojh@petrochina.com.cn (J.L.); dingb@petrochina.com.cn (B.D.); wangpm@petrochina.com.cn (P.W.); gengxf@petrochina.com.cn (X.G.)

² Key Laboratory of Nano Chemistry (KLNC), CNPC, Beijing 100083, China

³ Key Lab of Organic Optoelectronics & Molecular Engineering of Ministry of Education, Department of Chemistry, Tsinghua University, Beijing 100084, China; yichaoh@126.com

* Correspondence: jwzhang@dicp.ac.cn (J.Z.); yonggewei@mail.tsinghua.edu.cn (Y.W.); Tel.: +86-010-627-97852

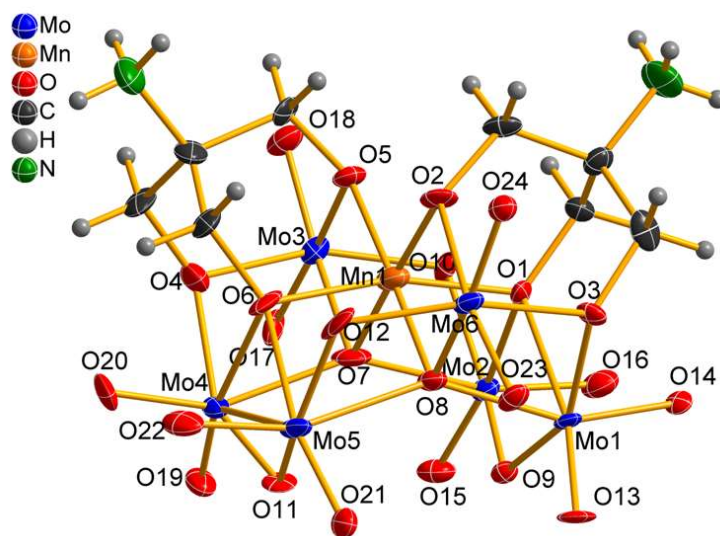
+ Y.H. and J.L. contributed equally to this work.

Table S1. Crystallographic data for compound **1**.

| Identification code | 1 |
|--------------------------------------|---|
| Empirical formula | C ₈ H ₂₂ N ₃ MnMo ₆ O ₂₄ |
| Formula weight | 1174.87 |
| Temperature (K) | 293 (2) |
| Crystal system | monoclinic |
| Space group | C2/c |
| a (Å) | 27.164(3) |
| b (Å) | 18.061(2) |
| c (Å) | 16.099(2) |
| α (°) | 90.00 |
| β (°) | 110.120(14) |
| γ (°) | 90.00 |
| Volume (Å ³) | 7416.4(15) |
| Z | 8 |
| Density (g.cm ⁻³) | 2.097 |
| μ (mm ⁻¹) | 2.369 |
| Crystal size (mm ³) | 0.55×0.50×0.40 |
| Reflections collected | 7199 |
| Independent reflections | 5784 |
| F (000) | 4448.0 |
| GOF | 1.084 |
| Final R indices [I > 2 σ (I)] | R ₁ =0.0535, wR ₂ =0.0974 |
| R indices (all data) | R ₁ =0.0596, wR ₂ =0.1012 |

$$^a R_1 = \frac{\sum ||F_o| - |F_c||}{\sum |F_o|}$$

$$^b wR_2 = \left\{ \frac{\sum [w(F_o^2 - F_c^2)^2]}{\sum w(F_o^2)^2} \right\}^{1/2}$$

Table S2. Selected bond lengths (Å) of cluster 1.

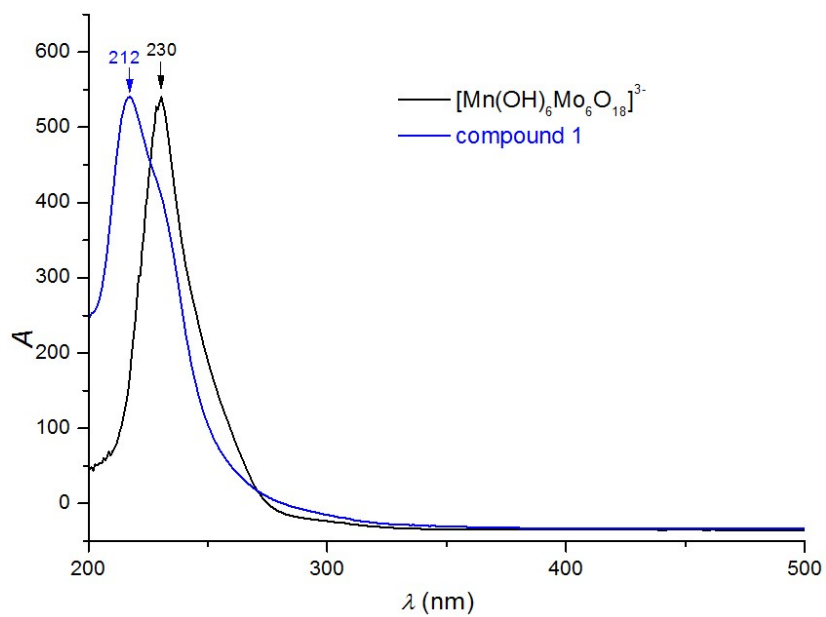
Selected bond lengths (Å) of cluster 1

| | | | |
|---------|-------|---------|-------|
| Mn1-O1 | 1.986 | Mo3-O10 | 1.904 |
| Mn1-O2 | 1.942 | Mo3-O17 | 1.698 |
| Mn1-O5 | 1.936 | Mo3-O18 | 1.728 |
| Mn1-O6 | 1.983 | Mo4-O4 | 2.098 |
| Mn1-O7 | 1.969 | Mo4-O6 | 2.280 |
| Mn1-O8 | 1.961 | Mo4-O7 | 2.160 |
| Mo1-O1 | 2.276 | Mo4-O11 | 1.882 |
| Mo1-O3 | 2.054 | Mo4-O19 | 1.693 |
| Mo1-O8 | 2.156 | Mo4-O20 | 1.722 |
| Mo1-O9 | 1.877 | Mo5-O6 | 2.315 |
| Mo1-O13 | 1.735 | Mo5-O8 | 2.262 |
| Mo1-O14 | 1.719 | Mo5-O11 | 1.914 |
| Mo2-O1 | 2.319 | Mo5-O12 | 1.944 |
| Mo2-O7 | 2.221 | Mo5-O21 | 1.691 |
| Mo2-O9 | 1.933 | Mo5-O22 | 1.701 |
| Mo2-O10 | 1.979 | Mo6-O2 | 2.189 |
| Mo2-O15 | 1.677 | Mo6-O3 | 2.145 |
| Mo2-O16 | 1.730 | Mo6-O8 | 2.169 |
| Mo3-O4 | 2.107 | Mo6-O12 | 1.899 |
| Mo3-O5 | 2.180 | Mo6-O23 | 1.712 |
| Mo3-O7 | 2.178 | Mo6-O24 | 1.732 |

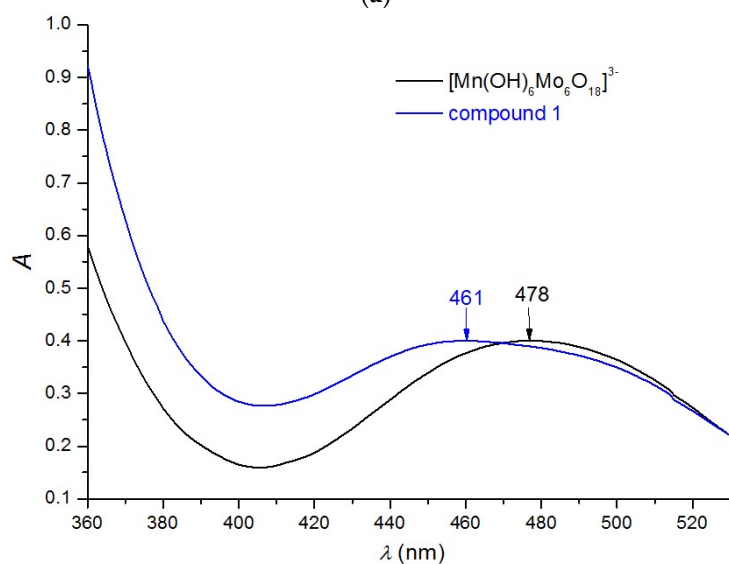
Table S3. Experimental hydrogen bonding interactions of compound **1**.

| Bond | H-Bonds | D–A [Å] | A···H [Å] | D–H···A [°] |
|----------|---------------|---------|-----------|-------------|
| 1 | N3–H3C····O14 | 2.897 | 2.247 | 138.52 |
| | N3–H3D····O11 | 2.900 | 2.206 | 145.00 |
| | N3–H3E····O15 | 2.992 | 2.211 | 168.11 |
| | N3–H3F····O19 | 2.719 | 2.468 | 99.54 |
| | N2–H2C····O16 | 3.483 | 2.959 | 119.46 |
| | N2–H2C····O24 | 3.453 | 2.793 | 132.19 |

The color of this Anderson β isomer triol functionalized derivative single crystal is different compared with Anderson α isomer triol functionalized derivative, because the color of the Anderson α isomer triol functionalized derivative was nearly the same as the normal α parent Anderson. The color of $[\text{Mn}(\text{OH})_6\text{Mo}_6\text{O}_{18}]^{3-}$ anion is orange while Anderson β isomer derivative (compound **1**) is dark orange. UV-Vis was applied for LMCT absorption and d-d transition absorption investigation. It should be noted that the UV-Vis spectra of such Anderson β isomer triol functionalized derivatives actually should be compared with the parent Anderson β isomer cluster, however such conjectured reaction intermediate has not yet been successfully obtained. As a compromise, we first compared them with the LMCT absorption band of the parent “Anderson–Evans”, $[\text{Mn}(\text{OH})_6\text{Mo}_6\text{O}_{18}]^{3-}$, locating around 230 nm which primarily corresponds to ligand centered $\mu_3\text{-OH}$ π to metal-centered $\text{Mo}^{6+} t_{2g}^*$ charge transfer transition (LMCT), these LMCT bands of compound **1** show hypsochromic shift to 212 ($\epsilon_{\text{LMCT}} = 5.31 \times 10^5 \text{ L}\cdot\text{mol}^{-1}\cdot\text{cm}^{-1}$, $7.42 \times 10^5 \text{ L}\cdot\text{mol}^{-1}\cdot\text{cm}^{-1}$ for parent Anderson cluster, compound **1**, respectively) It is due to the increase of crystal field splitting energy since the $\mu\text{-OCH}_2$ is stronger field ligand than that $\mu_3\text{-OH}$. The d-d transition absorption band of the parent $[\text{Mn}(\text{OH})_6\text{Mo}_6\text{O}_{18}]^{3-}$ locating around 478 nm is assigned to the metal centered lowest energy electronic transition from HOMO t_{2g}^* to LUMO e_g^* transition of Mn^{3+} . Similar hypsochromic shift phenomenon is observed in compound **1** at 461 nm, respectively ($\epsilon_{d-d} = 6.14 \times 10^2 \text{ L}\cdot\text{mol}^{-1}\cdot\text{cm}^{-1}$, $8.53 \times 10^2 \text{ L}\cdot\text{mol}^{-1}\cdot\text{cm}^{-1}$ for parent Anderson cluster, compound **1**, respectively). The hypsochromic shift is assigned to the reduction of charge density in $\mu\text{-O}$ when triol ligands anchored on. It is worthy to point out that in our previous work, similar range of hypsochromic shift was also observed in Anderson α isomer triol functionalized derivative, however, the ϵ_{LMCT} and ϵ_{d-d} is quite smaller. In fact, the ϵ_{LMCT} and ϵ_{d-d} of Anderson α isomer triol functionalized derivative is not much different from the parent Anderson α isomer $[\text{Mn}(\text{OH})_6\text{Mo}_6\text{O}_{18}]^{3-}$ anion. Thus, the color of the Anderson α isomer triol functionalized derivative and the corresponding parent cluster was nearly the same. Perhaps it is the total change of $\mu\text{-O}$ coordination environment in Anderson β isomer triol functionalized derivative skeleton that leads to the remarkable increase of ϵ_{LMCT} and ϵ_{d-d} and the related obvious color change.



(a)



(b)

Figure S1. (a) UV/Vis LMCT spectra of compound 1 and the flat Anderson-type POMs Cluster, $[\text{MnMo}_6\text{O}_{18}(\text{OH})_6]^{3-}$. (b) UV/Vis d-d transition spectra of compound 1 and the flat Anderson-type POMs Cluster, $[\text{MnMo}_6\text{O}_{18}(\text{OH})_6]^{3-}$.

Considering one of the obvious structure features in triol functionalized Anderson β isomer derivative is that there exist one type of μ_3 -O and two types of μ_2 -O, where triol ligand is anchored on their surface. Hence, there should be three different types of (μ -O-) C atoms where each carbon atom has different chemical shifts based on different electronegative environment according to dissimilar charge density of these μ -O atoms. In fact, the electronegative sequence of these μ -O atoms from stronger to weaker is as follows: μ_2 -O (coordinated one molybdenum atom and the central hetero atom) > μ_2 -O (coordinated with two molybdenum atoms) > μ_3 -O (coordinated with two molybdenum atoms and the central hetero atom). The ^{13}C NMR spectrum is another effective choice to verify such structure from another aspect. Thus, the ^{13}C NMR spectrum of compound **1** was conducted and all the peaks were clearly assigned to confirm the structure (Figure S2).

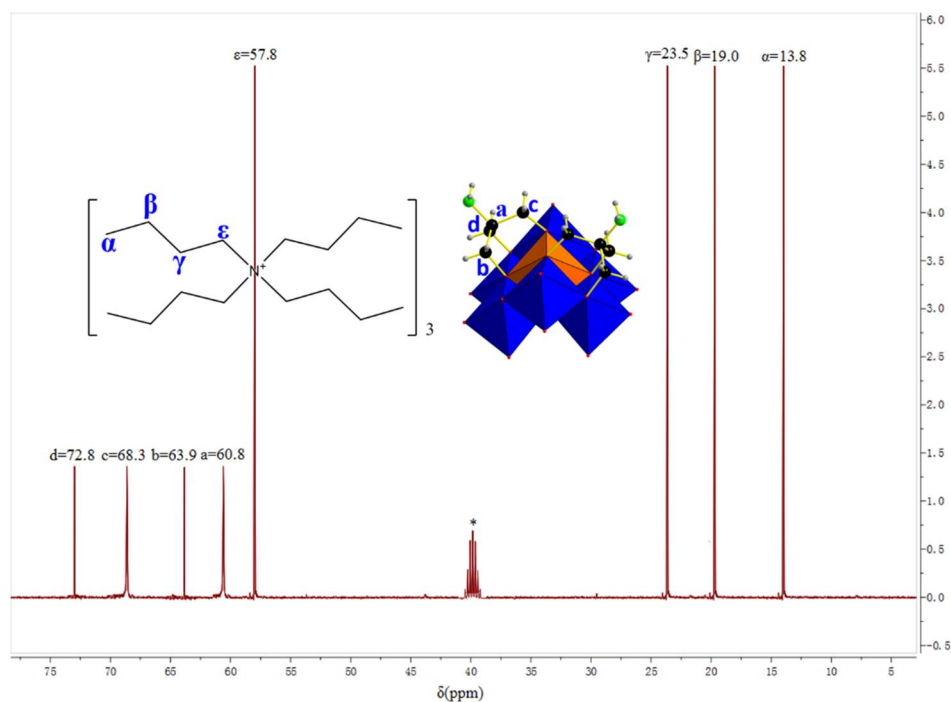
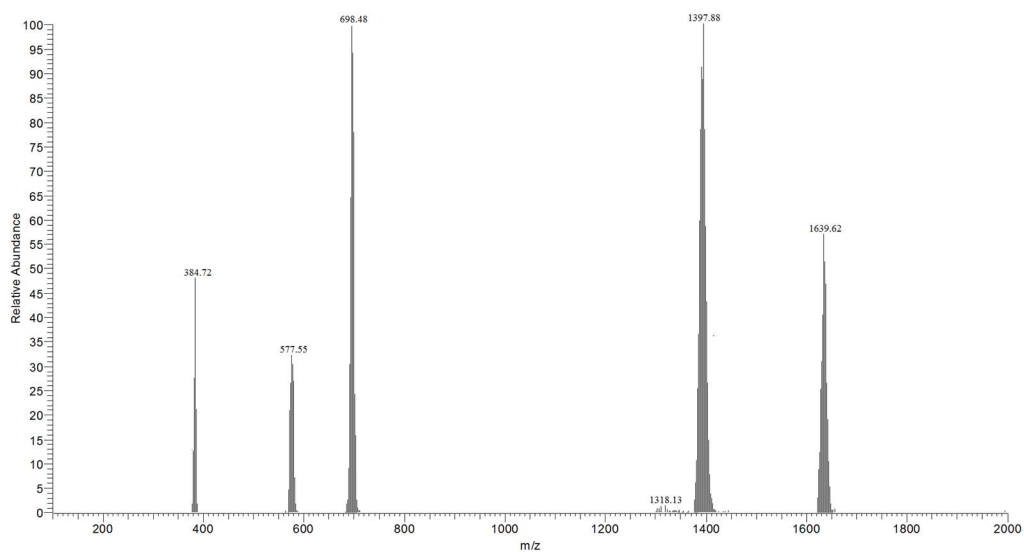
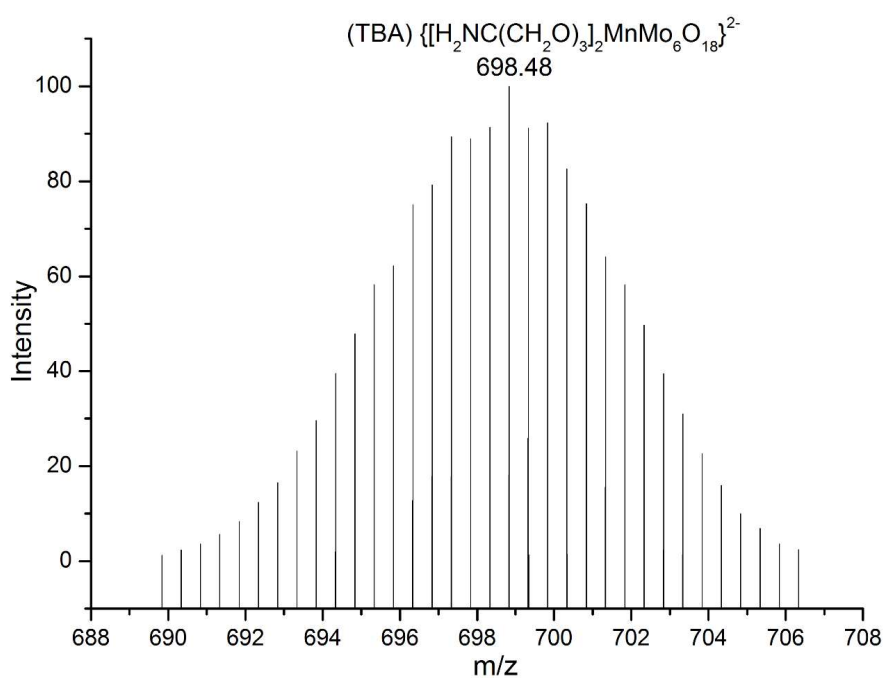


Figure S2. ^{13}C NMR spectrum of compound **1**.

The ESI-MS spectra of compound 1 was conducted and all the peaks the main peak with highest intensity and other identifiable peaks were clearly assigned to confirm the structure.



(a)



(b)

Figure S3. (a) ESI-MS of compound 1 with TBA⁺ cations. (b) ESI-MS of compound 1 with TBA⁺ cations (100% intensity peak in original size).

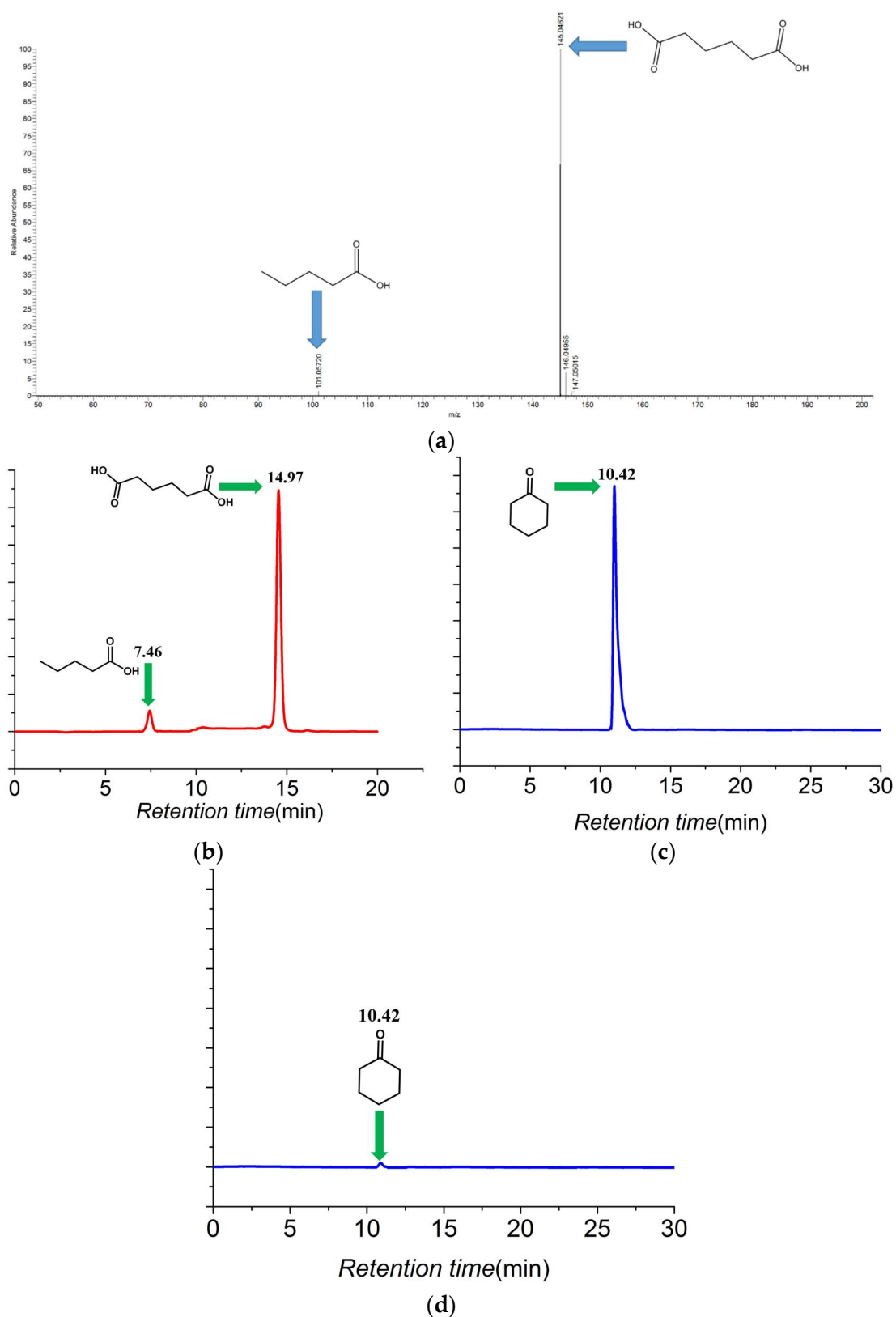
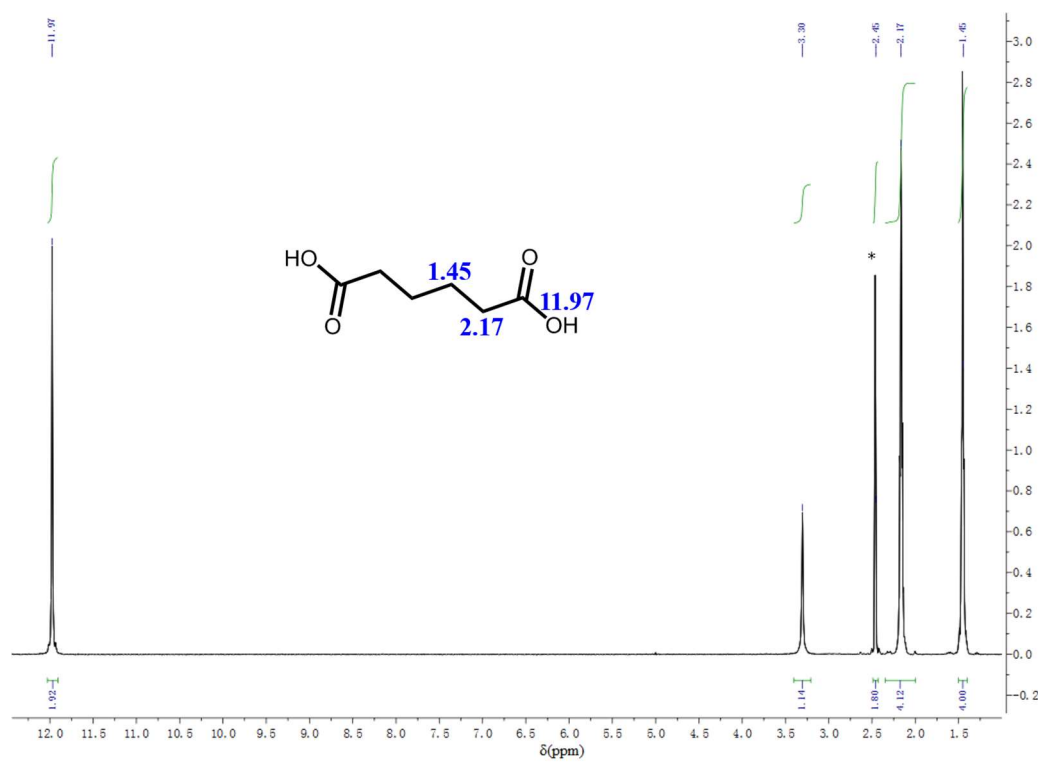
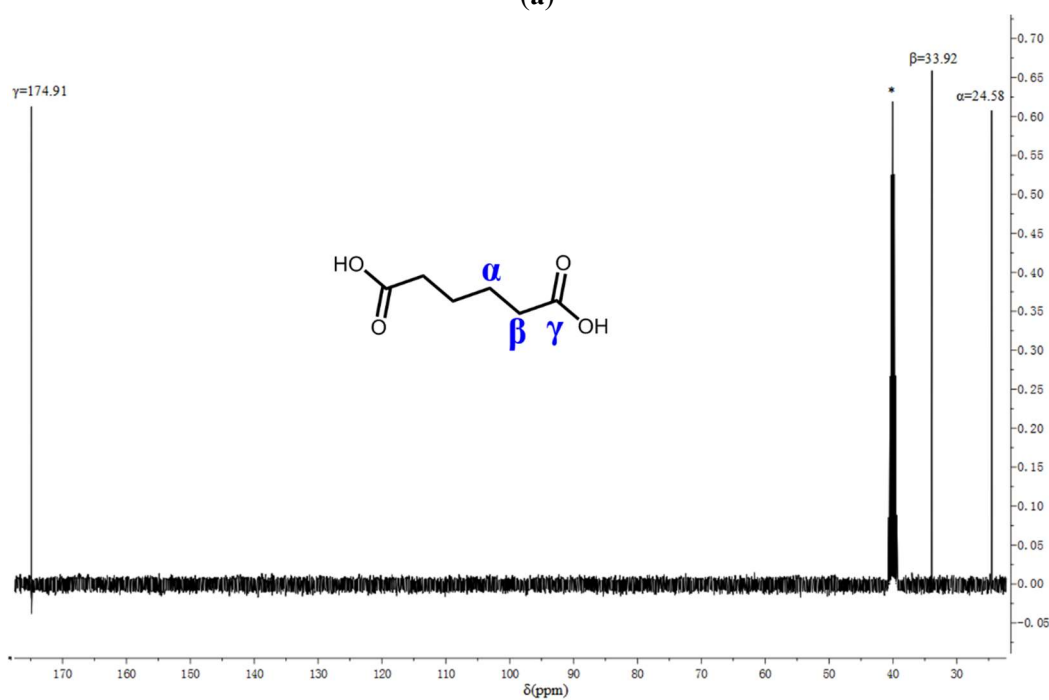


Figure S4. (a) The ESI-MS of white crystalline products generated from cyclohexanone in the presence of catalyst 1. (b) The HPLC retention time of white crystalline products dissolved in methanol. (c) The GC-MS of reaction solution dissolved in ethanol before catalytic reaction. (d) The GC-MS of reaction solution dissolved in ethanol after catalytic reaction.



(a)



(b)

Figure S5. (a) ¹H NMR spectrum of white crystalline product. (b) ¹³C NMR spectrum of white crystalline product.

Topology analysis of Catalysis Species

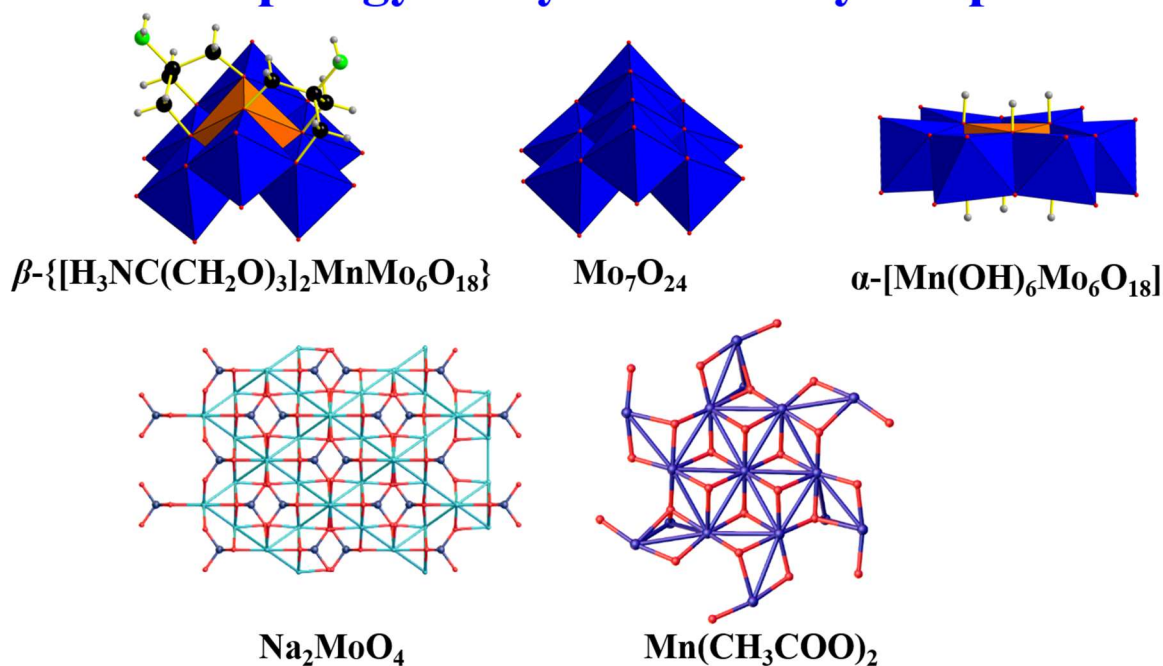


Figure S6. Topology analysis and comparison of Catalysis Species.

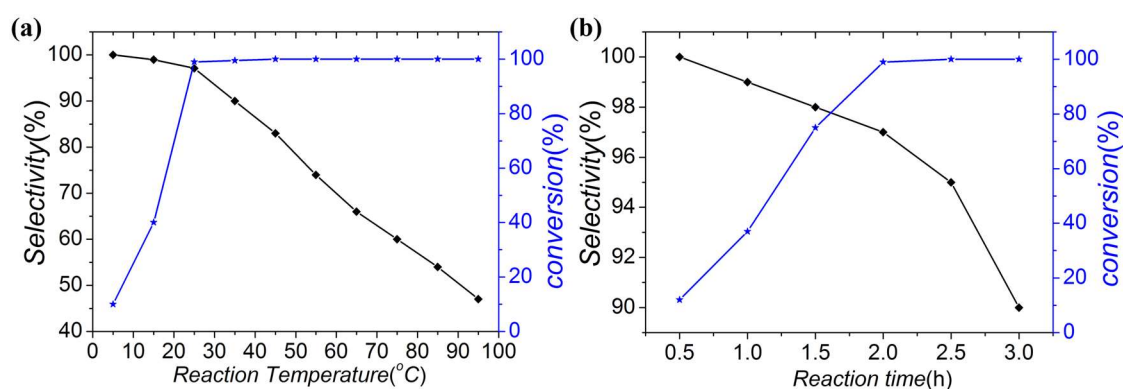


Figure S7. (a) The reaction selectivity and conversion versus reaction temperature, reaction condition catalyst (0.02 mol %), 30% H_2O_2 (100 mmol), DMSO (1 mmol), and cyclohexanone (30 mmol) at 2h. (b) The reaction selectivity and conversion versus time, reaction condition catalyst (0.02 mol %), 30% H_2O_2 (100 mmol), DMSO (1 mmol), and cyclohexanone (30 mmol) at 25°C in cyclohexanone oxidation catalytic reaction.

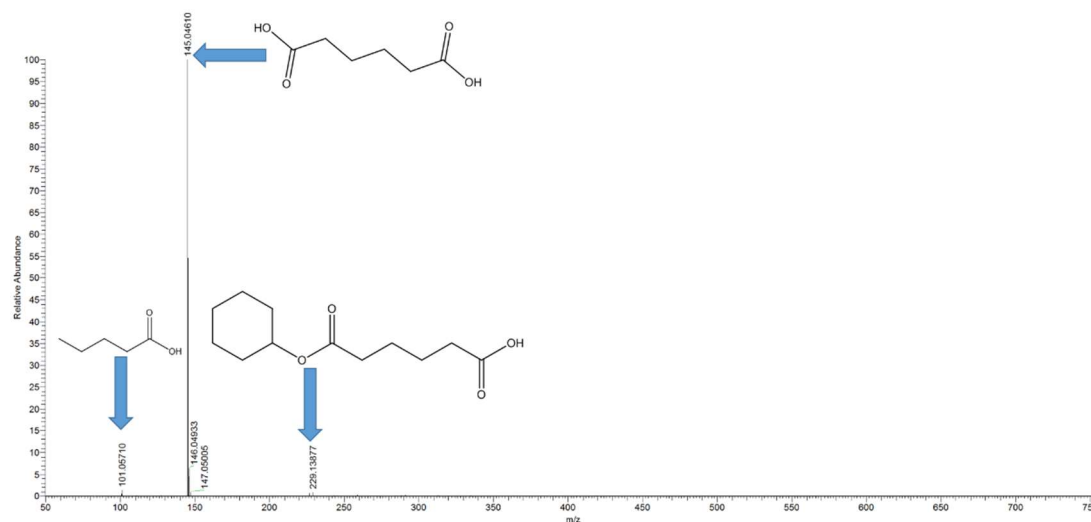


Figure S8. The ESI-MS of products from the catalytic oxidation of cyclohexanol at room temperature.

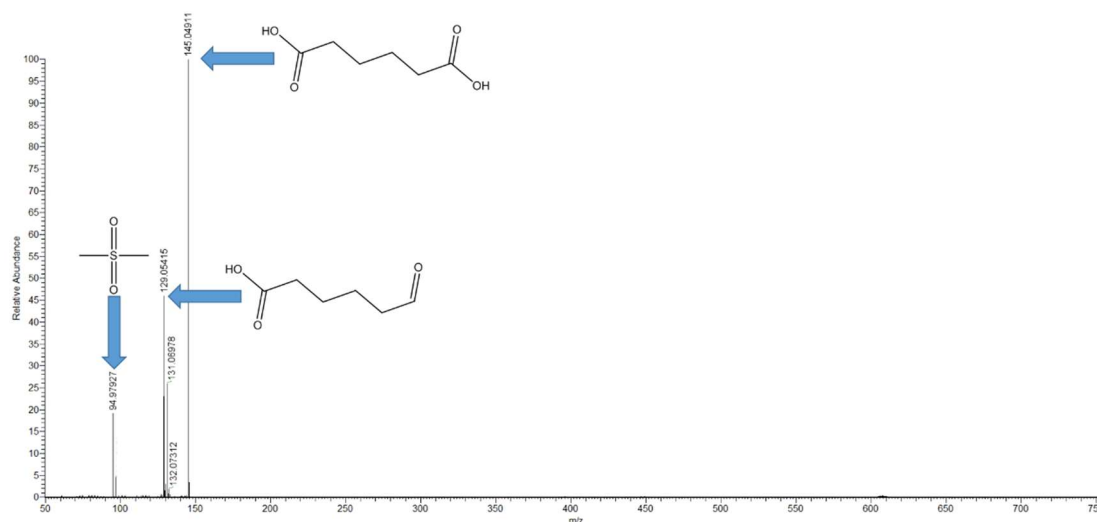


Figure S9. The ESI-MS of white crystalline products generated from cyclohexanol with DMSO.

© 2017 by the authors. Submitted for possible open access publication under the



terms and conditions of the Creative Commons Attribution (CC BY) license (<http://creativecommons.org/licenses/by/4.0/>).